Lysosomal Targeting of Cystinosin Requires AP-3

Zuzanna Andrzejewska[1,2], Nathalie Névo[1,2], Lucie Thomas[1,2], Anne Bailleux[1,2], Véronique Chauvet[1,2], Alexandre Benmerah[1,2] and Corinne Antignac[1,2,3,*]

[1]Inserm U1163, Laboratory of Hereditary Kidney Diseases, Paris, France
[2]Paris Descartes-Sorbonne Paris Cité University, Imagine Institute, Paris, France
[3]Assistance Publique - Hôpitaux de Paris (AP-HP), Department of Genetics, Necker Hospital, Paris, France
*Corresponding author: Corinne Antignac, corinne.antignac@inserm.fr

Abstract

Cystinosin is a lysosomal cystine transporter defective in cystinosis, an autosomal recessive lysosomal storage disorder. It is composed of seven transmembrane (TM) domains and contains two lysosomal targeting motifs: a tyrosine-based signal (GYDQL) in its C-terminal tail and a non-classical motif in its fifth inter-TM loop. Using the yeast two-hybrid system, we showed that the GYDQL motif specifically interacted with the μ subunit of the adaptor protein complex 3 (AP-3). Moreover, cell surface biotinylation and total internal reflection fluorescence microscopy revealed that cystinosin was partially mislocalized to the plasma membrane (PM) in AP-3-depleted cells. We generated a chimeric CD63 protein to specifically analyze the function of the GYDQL motif. This chimeric protein was targeted to lysosomes in a manner similar to cystinosin and was partially mislocalized to the PM in AP-3 knockdown cells where it also accumulated in the *trans*-Golgi network and early endosomes. Together with the fact that the surface levels of cystinosin and of the CD63-GYDQL chimeric protein were not increased when clathrin-mediated endocytosis was impaired, our data show that the tyrosine-based motif of cystinosin is a 'strong' AP-3 interacting motif responsible for lysosomal targeting of cystinosin by a direct intracellular pathway.

Cystinosin is a lysosomal cystine transporter encoded by the *CTNS* gene, mutations of which are responsible for cystinosis. It is a founding member of the 'PQ loop' protein family characterized by a seven-transmembrane (TM) domain structure and the presence of a duplicated 'PQ-loop motif' (1,2). Cystinosis is a rare autosomal recessive lysosomal storage disorder characterized by the accumulation of cystine in the lysosomes, which leads to the impairment of the function of multiple organs, including kidneys, endocrine glands, muscles and the central nervous system (3). The lysosomal localization of cystinosin was shown by confocal microscopy, using constructs encoding a wild-type (WT) cystinosin-enhanced green fluorescent protein (EGFP) fusion protein transfected in Madin-Darby Canine Kidney and *HeLa* cells (4). This localization could not be confirmed for endogenous cystinosin due to the lack of specific antibodies. However, endogenous cystinosin was later identified by mass spectrometry in a proteomic analysis of lysosomal membranes (5,6).

In agreement with its lysosomal localization, cystinosin is predicted to contain 7-*N*-glycosylation sites in the intraluminal amino-terminal region and a classical tyrosine-based lysosomal targeting signal fitting with the canonical GYXXØ sequence (Ø for hydrophobic residue) found in the short C-terminal cytosolic tail. Interestingly, the fifth inter-TM cytosolic loop has also been found to play a role in the lysosomal localization of cystinosin, as it comprises a novel, conformational targeting motif (4,7). These two signals play additive functions as deletion of the C-terminal tail or the fifth inter-TM loop of cystinosin leads only to partial relocalization of the protein to the plasma membrane (PM), whereas cystinosin is completely relocalized to the PM when both motifs are

altered (4). Subsequently, the presence of two lysosomal targeting motifs has also been described in CLN3 (neuronal ceroid-lipofuscinosis 3), a six-TM domain protein encoded by the gene mutated in Batten disease. As for cystinosin, both an unconventional signal and a classical dileucine motif were found to be important for the efficient lysosomal targeting of CLN3 (8).

Despite the identification of two lysosomal targeting signals within cystinosin, the cellular machineries responsible for the sorting and transport of this multispanning TM protein have not been characterized. Distinct adaptor protein complexes (AP-1 to AP-4 and probably the recently discovered AP-5), functioning at different donor membranes with or without clathrin, are involved in the selection of cargo molecules for vesicular transport via their ability to recognize specific sets of sorting motifs (7,9). They all share a heterotetrameric organization comprising two large subunits (adaptins: β1-5 and either γ, α, δ, ε or ζ, respectively), a medium subunit (μ1-5) responsible for tyrosine-based motif recognition and a small subunit (σ1-5). The AP complexes have different steady-state cellular localizations and different preferences for signal motif recognition, thus playing a role in TM protein trafficking to diverse organelles. The role of the newly described AP-5 complex in the trafficking of cargo molecules needs further elucidation (10).

Studies on lysosomal targeting of lysosome-associated membrane proteins (LAMPs), CD63 (late endosomal/lysosomal tetraspanin) and endolyn indicate the existence of different possible pathways by which proteins can be sorted to these organelles (11,12). The direct intracellular pathway involves sorting of neo-synthesized proteins from the *trans*-Golgi network (TGN) to the endosomal compartment from where they reach lysosomes. This pathway, during which proteins never reach the PM, was shown to depend on either AP-1, AP-3 or AP-4 (7,13). In the indirect pathway, proteins are transported from the TGN to the PM in an AP-independent mechanism and then internalized from the PM through clathrin-coated pits (AP-2-dependent mechanism), and further transported to endosomes and then lysosomes. The AP-2 complex participates only in the indirect pathway.

In this study, we aimed to decipher the mechanisms that control the proper sorting of cystinosin to the lysosomes. We first used the yeast two-hybrid system to identify the AP complexes that interact with the lysosomal targeting motifs of cystinosin. The effect of the identified AP complexes on the trafficking of cystinosin was further examined by cell surface biotinylation, total internal reflection fluorescence microscopy (TIRFM) and colocalization analysis. Finally, we analyzed the role of the intrinsic activity of the tyrosine-based motif of cystinosin using a chimeric CD63 protein where the endogenous tyrosine-based signal was replaced by that of cystinosin. Thus, our results show that cystinosin, by its strong interaction with the AP-3 complex, is targeted to the lysosomes mainly through the direct intracellular pathway, omitting the PM.

Results

Cystinosin cytosolic tail interacts with the μ subunit of AP-3 in the yeast two-hybrid system

We used the yeast two-hybrid system to identify the AP complexes that interact with the cystinosin tyrosine-based motif. As the interaction of sorting motifs with AP complexes can be dependent on surrounding amino acids (14), we used three different bait constructs corresponding to the cystinosin tyrosine-based motif fused to the DNA-binding domain of Gal4 including either the full-length C-terminal tail (RKRPGYDQLN) or the triple repeats of PGYDQL ((PGYDQL)x3) or of PGYDQLN ((PGYDQLN)x3) sequences. Similar constructs corresponding to the tyrosine-based lysosomal targeting signals of Lamp-1 (KRSHAGYQTI or (AGYQTI)x3) and CD63 (KSIRSGYEVM or (SGYEVM)x3) were used as controls. Moreover, we also tested the second unconventional lysosomal targeting motif of cystinosin present in the fifth inter-TM loop (KYFPQAYMNFYYKSTKGWS). The μ subunits of the AP complexes (μ1-4) together with the α-adaptin of AP-2, used here as a negative control, were cloned as fusion proteins with the transcriptional activation domain of Gal4 and their expression was verified by western blot (Figure 1A).

We verified if any of the fusion proteins expressed alone auto-activated the system by testing the ability of transformed cells to grow on histidine-restricted medium. Of all the constructs tested, only three ((SGYEVM)x3,

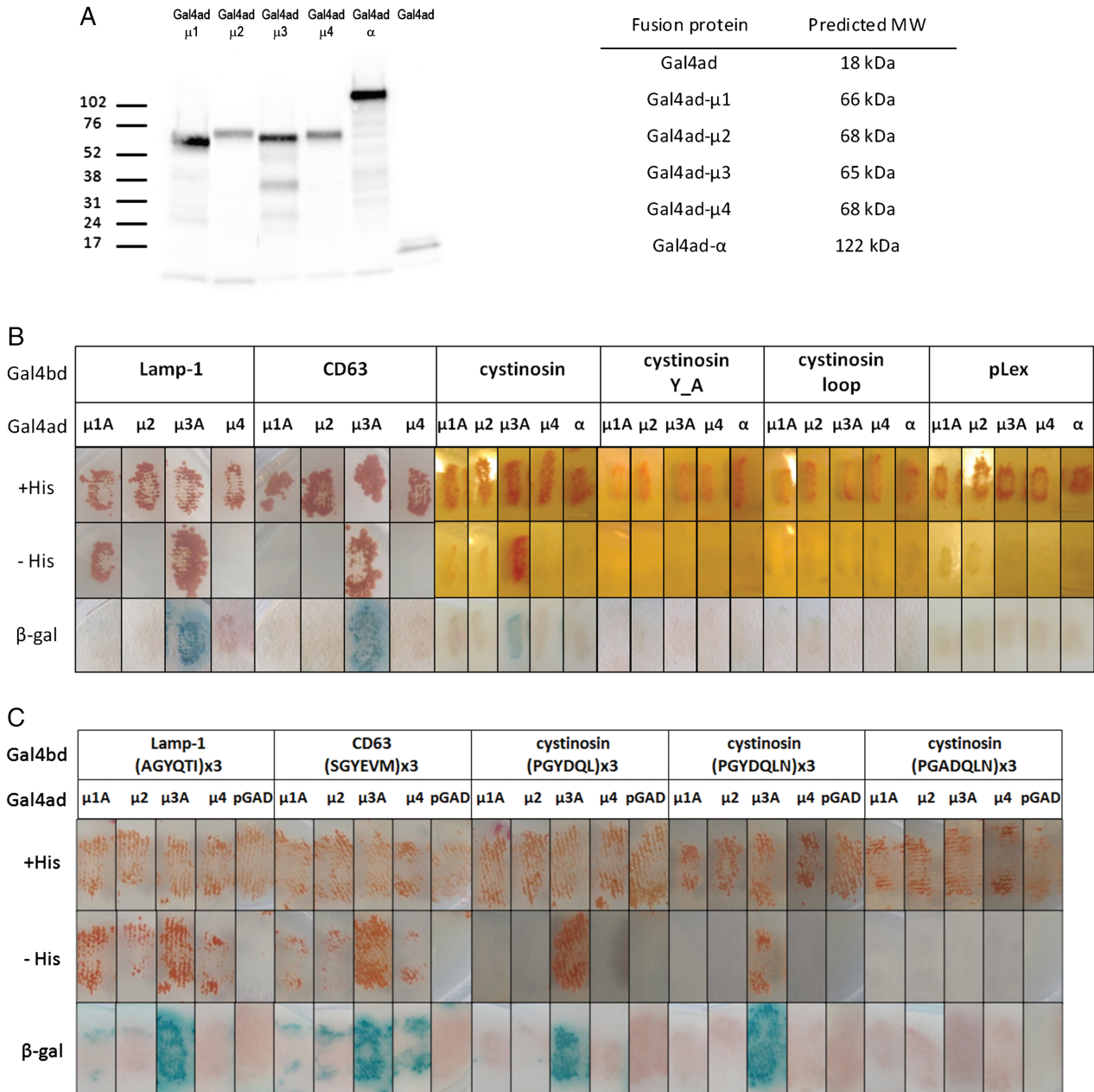**Figure 1:** **The cystinosin tyrosine-based motif interacts with the μ3 subunit of AP-3 in the yeast two-hybrid system.** A) The expression of all AP subunits fused to Gal4ad was analyzed by WB with an anti-Gal4-ad antibody. The predicted molecular weights of fusion proteins are listed in the table. B and C) Yeast cells were co-transformed with bait constructs (Gal4bd fusion) containing the full-length cytosolic tails of cystinosin, Lamp-1 or CD63 (B) or triple repeat of the tyrosine-based motif of Lamp-1 (AGYQTI), CD63 (SGYEVM), cystinosin (PGYDQL, PGYDQLN) or its mutated form (PGADQLN) (C) together with prey constructs (Gal4ad fusion) bearing subunits of AP complexes. Yeast transformants were tested for the ability to grow on histidine restricted medium and the β-galactosidase assay was performed to confirm the interactions. As selection in the absence of histidine alone was not sufficient to eliminate growth of the SGYEVMx3, PGYDQLx3 and PGYDQLNx3 co-transformed with the negative control plasmid pGAD, transformants containing these constructs were replicated on medium containing low concentration (2.5 mM) of 3-AT, competitive inhibitor of histidine biosynthesis.

(PGYDQL)x3 and (PGYDQLN)x3) induced the growth of some colonies on histidine-restricted medium, which was completely inhibited by addition of low doses of 3-aminotriazole (2.5 mM 3-AT; Figure S1), a competitive inhibitor of the HIS3 gene product widely used for background reduction, subsequently used for all experiments with the above described constructs in this study (14,15). The full-length C-terminal tail of cystinosin containing the GYDQL motif interacted only with the µ3 subunit. The substitution of alanine for the crucial tyrosine abolished the interaction confirming its specificity (Figure 1B). A strong interaction with µ3 was also detected for the C-terminal tails of Lamp-1 and CD63. No interaction was observed with the other µ subunits except for Lamp-1 with µ1 (Figure 1B). We then used constructs bearing triple repeats of the tyrosine-based motifs to enable detection of possible low affinity interactions with other µ subunits as successfully used for Lamp-1 by Ohno et al. (16). While interactions of Lamp-1 and CD63 with other µ subunits were detected in this context (µ2 and µ4; Figure 1C), the cystinosin tyrosine-based motif only interacted with the µ3 subunit regardless of the bait construct used ((PGY-DQL)x3 or (PGYDQLN)x3) and this interaction was dependent upon the tyrosine residue ((PGADQLN)x3) (Figure 1C). In addition, we did not observe any interaction between the second unconventional cystinosin loop motif with any of the µ subunits (Figure 1B), further confirming that the tyrosine residues of this domain are not part of a canonical tyrosine-based motif. Altogether, these results show that the GYDQL lysosomal targeting motif found in the C-terminal tail of cystinosin is a canonical tyrosine-based signal that specifically interacts with AP3.

AP-3 is responsible for efficient lysosomal sorting of cystinosin

Because we lack an antibody to detect endogenous cystinosin, we used the transient expression of cystinosin-EGFP fusion protein in *HeLa* cells as previously described (4). In line with what was already known about cystinosin localization in different cell lines (4), cystinosin-EGFP colocalized with the late endosomal-lysosomal markers Lamp-1 and CD63 in *HeLa* cells (Figure S2).

To test the role of the AP-3 complex in the trafficking of cystinosin, we generated stable *HeLa* cell lines transduced with lentiviral constructs containing short hairpin RNA targeting the δ subunit of AP-3 (shAP-3) or Luciferase (shLuc) as control. This led to a strong decrease of the expression of the δ subunit detected both by western blotting (WB) (∼75%; Figure S3A) and by immunofluorescence (IF) (Figure S3B), whereas the expression of AP-2 and AP-1 subunits remained unchanged (Figure S3A). Increased levels of cargoes at the PM in AP-3-deficient cells have been widely used as a reliable readout for AP-3 function (17–19). Flow cytometry analyses of non-permeabilized *HeLa* shAP-3 cells showed a moderate increase in surface levels of CD63 and Lamp-1 but not of the transferrin receptor (TfR) (Figure S3C,D). These results were similar in range to previously published ones (18,20,21) and therefore validate the functional knockdown of the AP-3 complex in our shAP-3 cell line.

We first used cell surface biotinylation to determine the possible mislocalization of WT or mutant forms of cystinosin to the PM in AP-3-depleted cells. As expected, in control cells, both the fifth loop (ΔYFPQA) and the tyrosine-based motif (ΔGYDQL) deletion mutants of cystinosin showed increased biotinylation compared to WT, with a more pronounced effect for the mutant of the tyrosine-based motif (Figure 2A,B). Furthermore, cell surface expression of WT cystinosin-EGFP was significantly increased in *HeLa* shAP-3 cells (Figure 2A,B). We also observed a trend, although not significant, in the AP-3 dependent increase of surface levels of the ΔYFPQA-EGFP mutant. As expected, no difference was visible for the ΔGYDQL-EGFP protein (Figure 2A,B). These data support the hypothesis that cystinosin is delivered to lysosomes in an AP-3-dependent manner and indicate the importance of the C-terminal targeting motif in this pathway. To confirm the biotinylation results, cell surface-associated cystinosin was analyzed by TIRFM that allows excitation of fluorophores found in close proximity to the adherent PM. As WT cystinosin was expected to be absent from the PM and therefore poorly detectable by TIRFM, which was indeed the case (Figure 2C), cells were co-transfected with a plasmid encoding farnesylated monomeric DsRed (DsRed-Monomer-F) used as a PM marker as previously described (22). Co-expression of cystinosin was verified by epifluorescence before TIRFM acquisition (Figure S4). As in the biotinylation study, we observed a strong increase in the cell surface expression

of the two mutants (ΔYFPQA and ΔGYDQL) compared to WT cystinosin. We also observed an almost twofold increase in the cell surface expression of WT cystinosin in *HeLa* shAP-3 cells (Figure 2C,D). Altogether, these results show that impairment of the interaction of cystinosin with AP-3 results in its misrouting to the cell surface.

Even though we did not observe the interaction of neither of the cystinosin motifs with µ2 in the yeast two-hybrid study, to rule out the possibility of indirect effect of AP-2-dependent internalization on cystinosin trafficking, we generated *HeLa* cell line depleted for AP-2 (shAP-2) using a short hairpin RNA targeting the µ2 subunit. Expression of the AP-2 complex in this cell line was specifically and strongly decreased as observed by WB for µ2 (~75%; Figure S3A) as well as by IF staining for the α-adaptin (Figure S3B). As for AP-3 depletion, we analyzed the cell surface expression of endogenous CD63, Lamp-1 and TfR in *HeLa* shAP-2 cells by flow cytometry (Figure S3C). As expected from previous studies (18,23,24), cell surface expression of all these proteins was strongly increased in shAP-2 cells (Figure S3C). Moreover, internalization of transferrin (Tf), the widely used marker of clathrin-mediated endocytosis, was also highly impaired in these cells (Figure S3D). As for AP-3, we used TIRFM and cell surface biotinylation to analyze the effect of AP-2 depletion on the expression of cystinosin at the PM. We could not observe any increase of PM expression for any of the cystinosin fusion proteins in AP-2-depleted cells compared to control cells (Figure 3). Altogether with the AP-3 data, these results indicate that cystinosin is very likely delivered to the lysosomes via a direct AP-3-dependent pathway, bypassing the PM.

The cystinosin tyrosine-based motif is a 'strong' AP-3 motif

The targeting of CD63 is strictly dependent on a unique tyrosine-based motif (GYEVM) in its C-terminal tail that interacts mainly with AP-3 and to a much lesser extent with AP-2 (12). To better analyze the importance of the C-terminal tyrosine-based motif of cystinosin in the targeting process, we generated an EGFP-CD63 chimeric protein in which the endogenous C-terminal tail of CD63 was replaced by that of cystinosin (EGFP-CD63-Cter) (Figure 4A). When transiently expressed in *HeLa* cells, both EGFP-CD63-Cter and EGFP-CD63 colocalized with

Lamp-1 (Figure 4B, arrows), showing efficient delivery of these fusion proteins to the late endosomal/lysosomal compartment. As already described (12,25), EGFP-CD63 was also found at the PM where it colocalized with wheat germ agglutinin (WGA), a lectin that selectively binds to glycosylated proteins (Figure 4C, arrowheads). Interestingly, colocalization with WGA was not observed for WT cystinosin or for the CD63-Cter fusion proteins (Figure 4C). These results were further confirmed by TIRFM. As shown in Figure 5, in contrast to cystinosin, CD63 was clearly detected at the PM. We observed much lower levels of EGFP-CD63-Cter at the cell surface compared to EGFP-CD63 (Figure 5), suggesting that the GYDQL motif of cystinosin efficiently prevents the delivery of CD63 at the PM. Using this system, we also further confirmed the effect of AP-3 on the trafficking properties of the cystinosin tyrosine-based motif. Similarly, as for WT cystinosin-EGFP, we observed an increase in the level of the EGFP-CD63-Cter at the PM in *HeLa* shAP-3 cells (Figure 5A,B). Surprisingly, we did not observe increased surface levels of EGFP-CD63 in AP-3-depleted cells. In our study, stable AP-3 depletion does not severely affect trafficking of endogenous CD63 (Figure S3C), similar to what was published using transient knockdown with siRNA (18,20) or AP-3-deficient cells from *pearl* mice (21). It is thus likely that this small increase could not be detected by TIRFM for the EGFP-CD63 protein as its surface expression is already high in control cells. However, AP-2 depletion resulted in an increased cell surface expression of EGFP-CD63 (Figure 5C,D), as expected from observed high levels of endogenous CD63 in these cells (Figure S3C) (18), but it did not affect the trafficking of the EGFP-CD63-Cter chimera (Figure 5C,D). These latter results further indicate that the AP-2 complex is not involved in the trafficking of cystinosin to the lysosomes which very likely does not follow the indirect route via the PM.

In agreement with an AP-3-dependent intracellular sorting pathway, we observed an increased colocalization of cystinosin-EGFP and EGFP-CD63-Cter with TGN46 in *HeLa* cells depleted of AP-3, indicating accumulation of these proteins in the TGN (Figure 6A). We also analyzed the localization of both proteins in early endosomes using early endosome antigen 1 (EEA1) as a marker of these organelles. We observed a higher
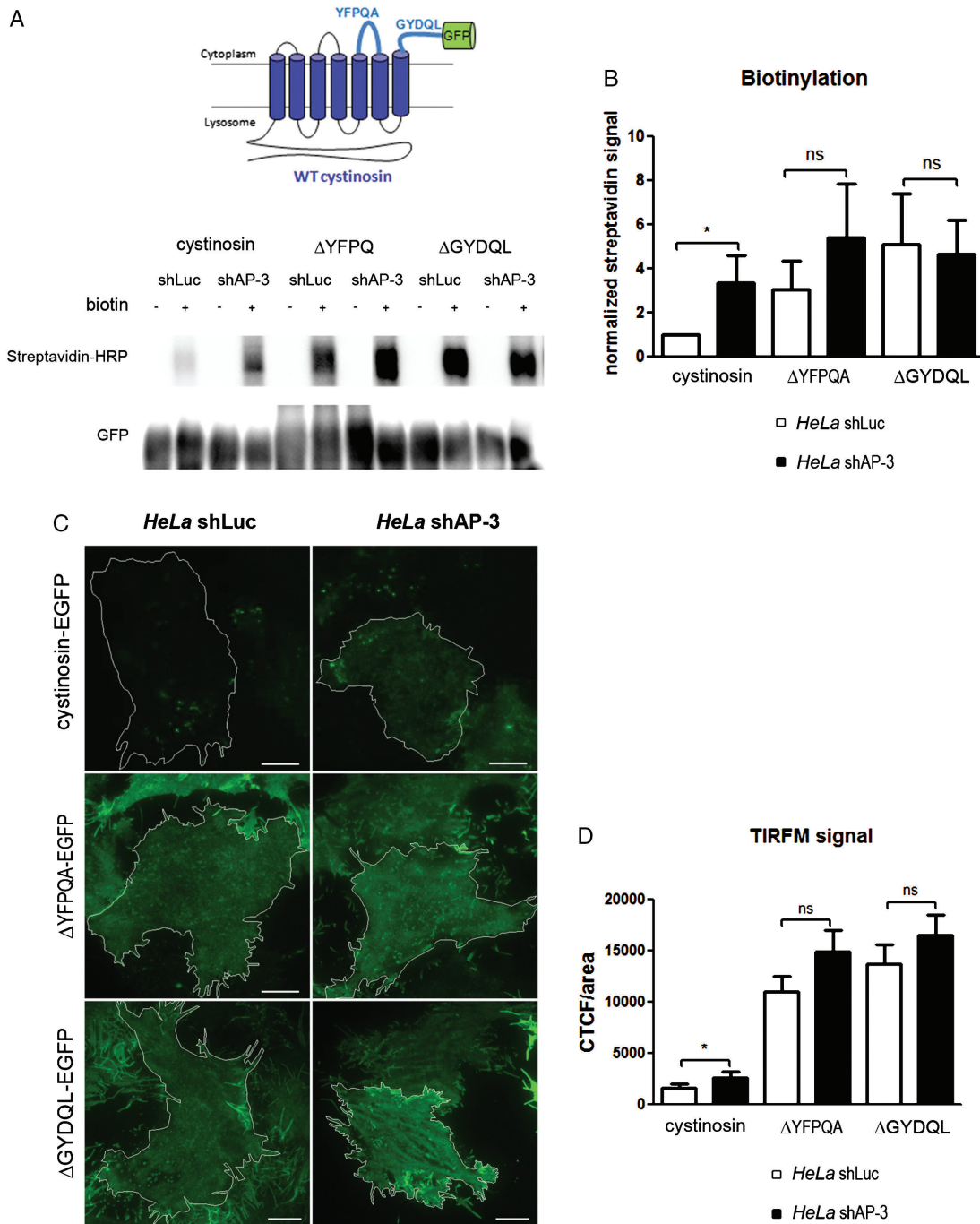
Figure 2: Cystinosin lysosomal targeting is dependent on the AP-3 complex. Control and AP-3-depleted *HeLa* cells were transfected with cystinosin-EGFP, ΔGYDQL-EGFP or ΔYFPQA-EGFP. A) Non-permeabilized cells were biotinylated in order to label proteins at the cell surface. Lysates were immunoprecipitated with anti-GFP antibody and immunoprecipitated proteins were analyzed by WB with streptavidin-HRP and anti-GFP antibody. Representative blots from at least three independent experiments are shown. B) Quantification of the biotinylation signal; $n = 4$ (*$p < 0.05$; ns, non-significant). C) The analysis of cell surface-associated cystinosin was performed 20 h after transfection by TIRFM on living cells co-expressing DsRed-F (see *Materials and Methods*); scale bars = 10 μm. D) Quantification of the PM signal is represented as CTCF/area; $n = 3$ (*$p < 0.05$, each bar represents the mean with SEM of at least 15 cells).
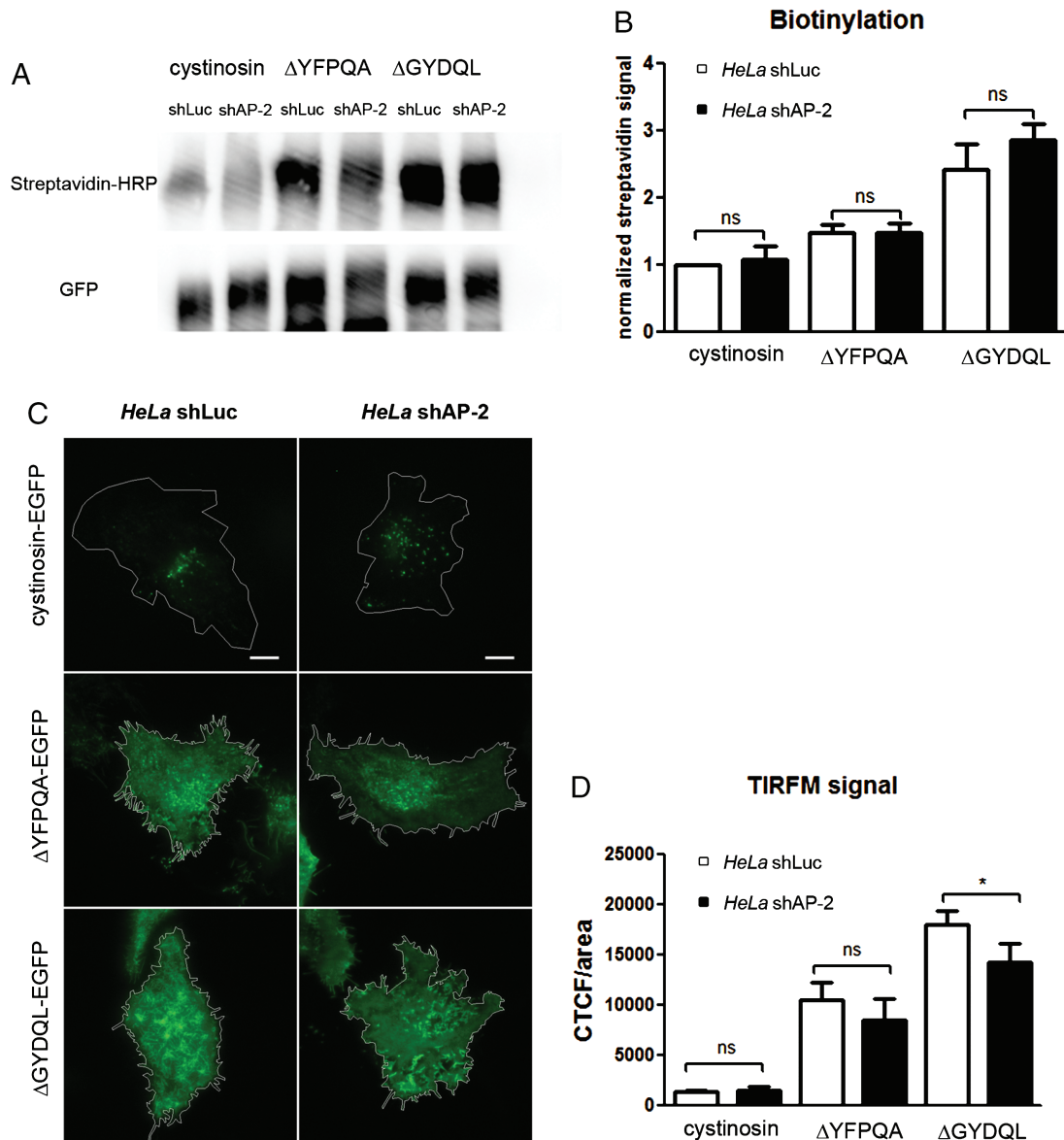
Figure 3: Cystinosin does not accumulate at the PM in AP-2-depleted cells. Control and AP-2-depleted *HeLa* cells were transfected with cystinosin-EGFP, ΔGYDQL-EGFP or ΔYFPQA-EGFP. A) Non-permeabilized cells were biotinylated 20 h after transfection in order to label surface proteins. The immunoblots of EGFP-immunoprecipitated proteins were revealed with streptavidin-HRP and anti-GFP antibody. Representative blots from at least three independent experiments are shown. B) Quantification of biotinylation signal; $n = 3$. C) Analysis of cell surface cystinosin signal was performed 20 h after transfection by TIRFM in living cells as in Figure 2 (scale bars = 10 μm). D) Quantification of PM signal was performed represented as CTCF/area; $n = 3$ (*$p < 0.05$; ns, non-significant, each bar represents the SEM of at least 15 cells).

degree of colocalization of EGFP-CD63-Cter with EEA1 in *HeLa* cells depleted of AP-3 (Figure 6B). Altogether, these results further indicate that cystinosin follows an AP-3-dependent intracellular pathway for lysosome delivery.

Discussion

Even though the extensive study of lysosomal proteins resulted in the description of a broad spectrum of targeting motifs, the trafficking of multispanning TM proteins
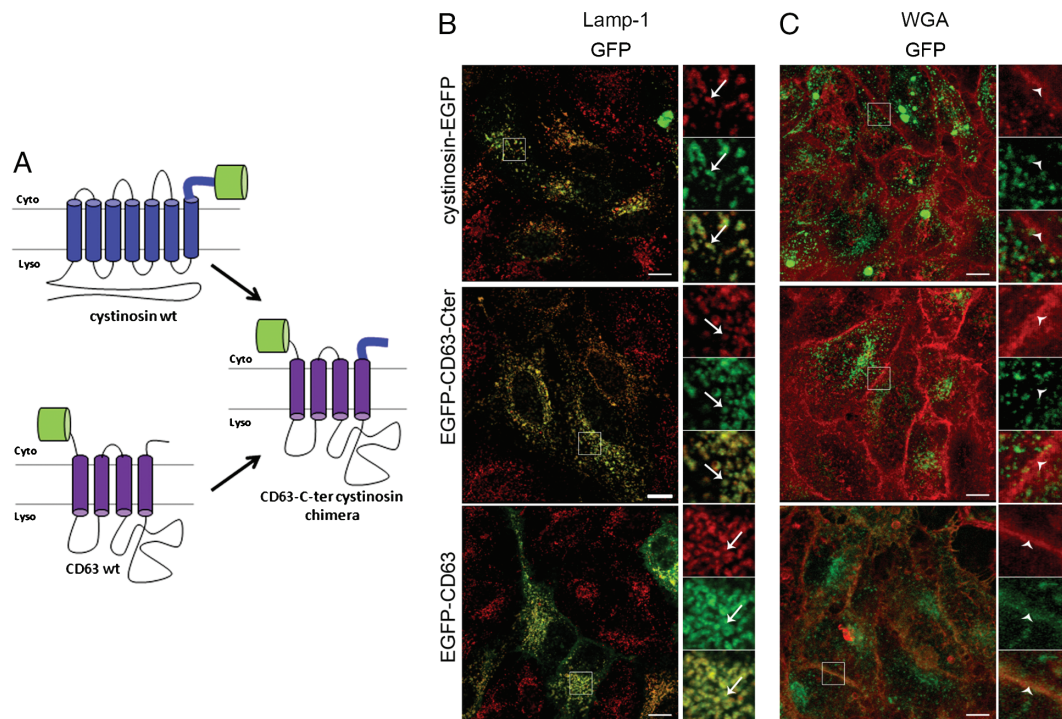
Figure 4: The C-terminal tyrosine-based signal of cystinosin is a lysosome targeting signal. A) Schematic representation of the EGFP-CD63 chimera. B and C) *HeLa* cells transiently expressing cystinosin-EGFP, EGFP-CD63 or EGFP-CD63-Cter proteins were labeled with Lamp-1 (lysosomal marker) (B; red) or WGA (PM marker) (C; red). Arrows and arrowheads indicate lysosomal and PM localization respectively (scale bars = 10 μm).

remains incompletely understood. The lysosomal targeting of cystinosin, a seven-TM protein, had been found to be dependent on two sorting signals: a canonical tyrosine-based motif (GYDQL) and a non-classical motif in its fifth-inter TM loop (4). The C-terminal signal of cystinosin presents all characteristics of classical tyrosine-based YXXØ-type lysosomal targeting motifs, which are typically found at the C-terminal end close to the TM domain (∼6–13 amino acids from TM). Moreover, according to the known preference of each μ subunit of the AP complexes for specific amino acids within the signal, it was likely that the GYDQL motif would be recognized by the AP-3 complex since the μ3 subunit prefers a G residue at the Y-1 position and the presence of acidic amino acids after the Y (26), and the GYDQL sequence of cystinosin fits both of these criteria. Indeed, in the yeast two-hybrid system, we were able to show the specific interaction of cystinosin C-terminal tail with the μ3 subunit. Moreover, we showed that this interaction was sustained when constructs bearing the motif sequence

without the larger tail context (PGYDQL or PGYDQLN) were used. This reflects the high affinity of the cystinosin tyrosine-based motif for AP-3, which is not influenced by the neighboring tail sequence or the presence of an additional residue after the bulky hydrophobic amino acid (Ø). From the strong affinity of GYDQL for only the AP-3 complex, we hypothesized that this motif could be implicated in the intracellular targeting of cystinosin. Effectively, while cystinosin-EGFP was not detected at the PM in control *HeLa* cells, it was partially mislocalized to the PM in AP-3-depleted *HeLa* cells as could be shown by cell surface biotinylation experiments and TIRFM analysis.

While our data clearly established that the C-terminal GYDQL motif is a 'strong' AP-3-dependent motif (see also below), the fact that cystinosin variants presenting a deletion of either the fifth loop or the C-terminal motif are still present at lysosomes indicates that each motif provides independent information for lysosomal targeting (4). In favor of this idea is the observed steady-state localization
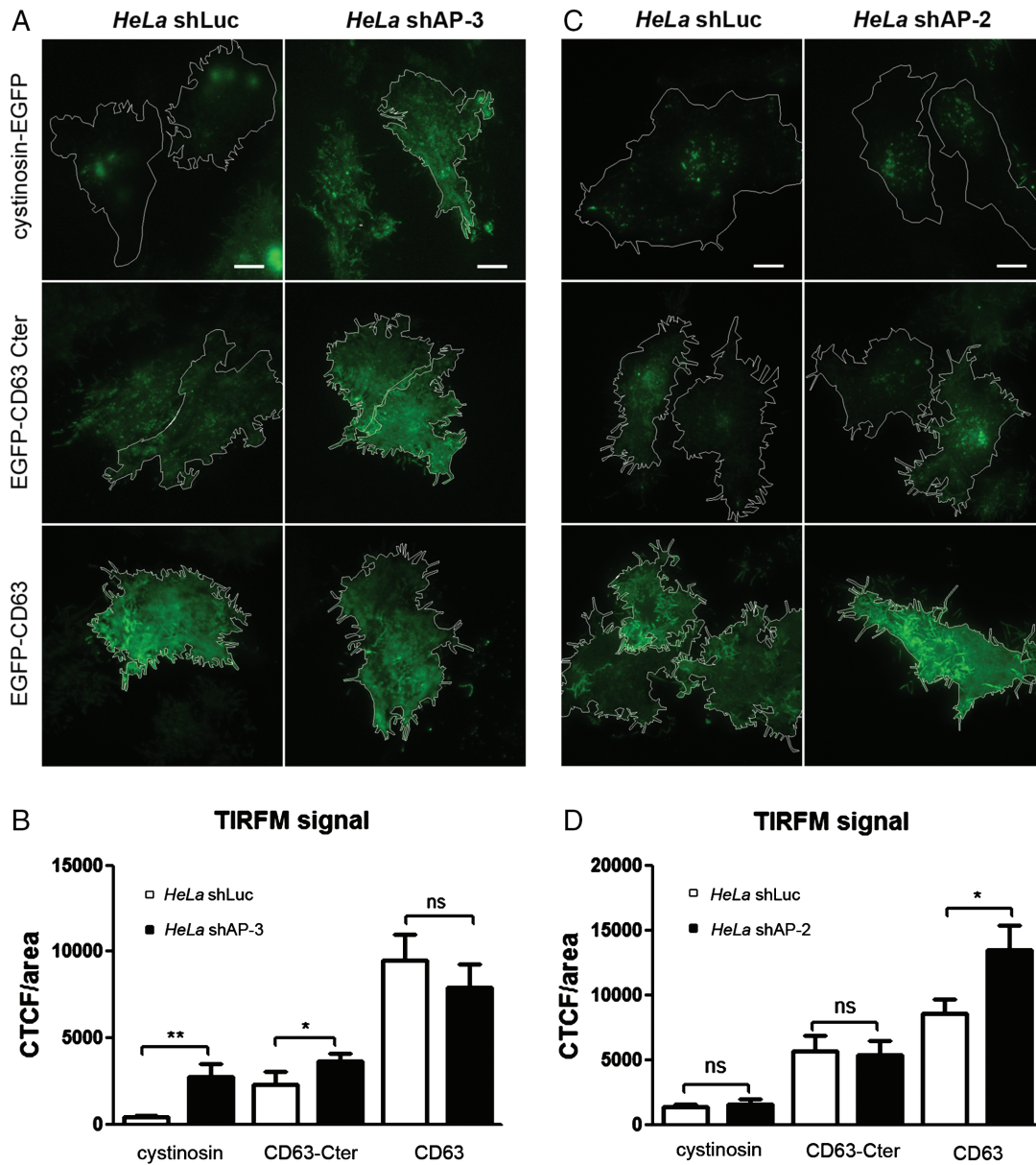
Figure 5: EGFP-CD63-Cter trafficking depends on AP-3. A–D) Control (shLuc), AP-2 (shAP-2) and AP-3 (shAP-3)-depleted *HeLa* cells were transfected with cystinosin-EGFP, EGFP-CD63-Cter or EGFP-CD63. A and C) The analysis of cell surface signal of GFP fusion proteins was performed 20 h after transfection by TIRFM in living cells as in Figure 2 (scale bars = 10 μm). B and D) Quantification of cell surface signal was performed as in Figure 3; $n = 3$ (B), $n = 2$ (D) (*,**$p < 0.05$; ns, non-significant, each bar represents the SEM of at least 10 cells).

of the cystinosin-LKG isoform (27). An alternative splicing of *CTNS* mRNA results in the expression of a longer cystinosin isoform in which the last C-terminal amino acids of cystinosin (including YDQLN) are replaced by a 38 amino acid-long sequence (LQAARTGSGSRLRQDWAP-SLQPK ALPQTTSVSASS*LKG*). This isoform was shown to

be localized to a wide spectrum of intracellular compartments such as lysosomes, multivesicular bodies, Golgi and endoplasmic reticulum along with the PM (27). The fact that this isoform lacking the GYDQL motif is expressed at the PM, which is not observed for the main classical isoform of cystinosin, further indicates the importance of
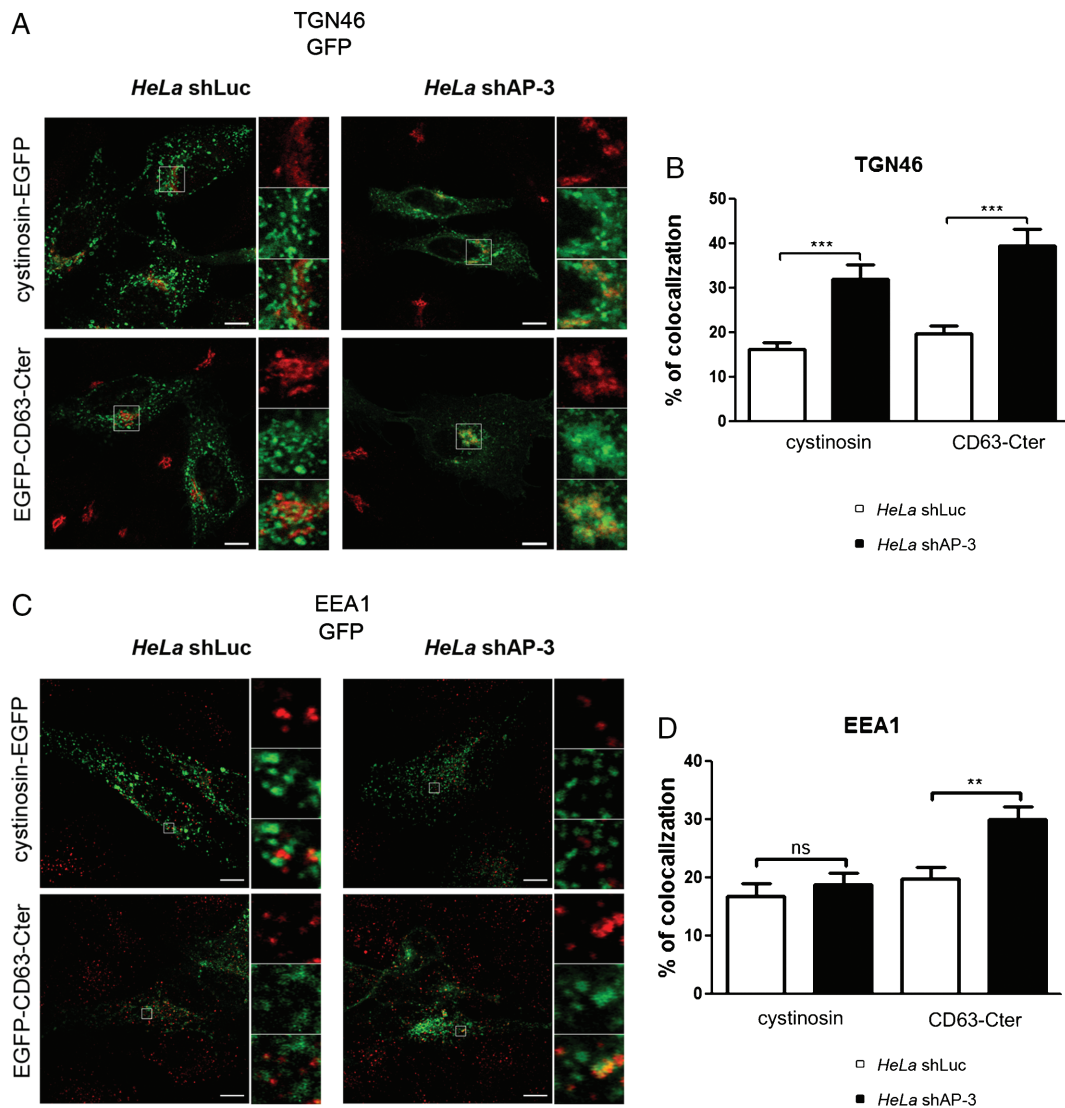
Figure 6: EGFP-CD63-Cter accumulates in the *trans*-Golgi and early endosomal compartment in the absence of AP-3.
A–D) Control (shLuc) and AP-3 (shAP-3)-depleted *HeLa* expressing cystinosin-EGFP or EGFP-CD63-Cter proteins were co-labeled with TGN46 (A; red) or EEA1 (C; red). B and D) The percentage of colocalization between each fusion protein and TGN46 (B) or EEA1 (D) was analyzed with the IMAGEJ 1.47 software; $n = 3$ (B), $n = 2$ (D) (**p < 0.05, ***p < 0.0001; each bar represents the SEM of at least 20 cells).

this sequence in direct intracellular lysosomal targeting. Moreover, although cystinosin-LKG does not comprise any known classical lysosomal targeting motif in its specific added sequence, it still contains the second unconventional targeting signal in its fifth loop (4,27). Additional investigation will be required to decipher the exact mechanism of action of this non-classical loop motif. Indeed, despite the presence of tyrosines, no interaction of the fifth loop motif with any of the µ subunits could be detected in the yeast

two-hybrid system and its activity was not perturbed in AP-3- or AP-2-depleted cells, indicating that its role in the trafficking of cystinosin is independent of µ subunit-based recognition mechanisms.

To better analyze the specific contribution of the GYDQL motif in the trafficking of cystinosin, beyond the context of the fifth loop motif, we generated a CD63 chimeric protein containing the C-terminal tail of cystinosin instead of

that of the WT protein (EGFP-CD63-Cter). Overexpressed WT CD63 was shown to localize to the endo-lysosomal compartment as well as to the PM (12,25). Moreover, decreased PM expression was shown for the CD63 protein when the last M of the SGYEVM motif was mutated into I (12). The trafficking of the CD63 form with the SGYEVI motif was exclusively dependent on AP-3 and no longer on AP-2 (12). Strikingly, we observed a similar effect on the subcellular distribution of CD63 when we exchanged its C-terminal sequence with that of cystinosin (EGFP-CD63-Cter). Although the EGFP-CD63 protein was localized to the endo-lysosomal compartment and the PM in *HeLa* cells, the EGFP-CD63-Cter showed decreased levels at the PM and colocalized extensively with Lamp-1. In addition, the EGFP-CD63-Cter levels at the PM were increased in an AP-3-dependent manner. Moreover, we could observe the accumulation of EGFP-CD63-Cter protein in the *trans*-Golgi and early endosomal compartments in AP-3-depleted cells. No accumulation in early endosomes could be observed for cystinosin-EGFP most likely because of the autonomous activity of the motif present in its fifth loop. Altogether, the data obtained from the analysis of the localization of the chimeric protein further confirm that the cystinosin tyrosine-based motif strongly interacts with AP-3 and that this interaction plays an important role in cystinosin lysosomal targeting via an intracellular pathway. So far, contradictory studies exist with regard to the exact intracellular compartment on which the recognition of AP-3 cargo takes place and AP-3-positive vesicles were proposed to bud from both TGN and EEs (11,12,28). Thus, cystinosin might reach late endosomes/lysosomes directly from TGN and/or by passing (from the verb to pass and not to bypass) through early endosomal compartment and our results are compatible with both of these hypotheses.

PQLC2/LAAT-1, a new lysosomal transporter of cationic amino acids belonging to the PQ-loop protein family, has recently been identified (1,29). PQLC2/LAAT-1 shares a seven-TM organization with cystinosin and its lysosomal targeting was shown to be dependent on an acidic dileucine AP-binding motif present in its C-terminal tail. Substitutions of both crucial leucine residues of the motif lead to the mislocalization of the protein to the PM (1). It would be interesting to further verify the manner in which PQLC2/LAAT-1 is delivered to lysosomes and thus if the targeting via a direct AP-3-dependent pathway constitutes a more general mechanism used by the multispanning lysosomal amino acid transporters.

Materials and Methods

Reagents

Reagents were obtained from the following sources: antibodies to human CD63 (H5C6) and human Lamp-1 (H4A3) from Developmental Studies Hybridoma Bank, antibody to TGN46 from Abcam, antibodies to AP50, adaptin-δ and adaptin-γ from BD Biosciences, antibodies to TfR (CD71; DF1513) and α-adaptin (C-18; AP-2) from Santa Cruz Biotechnology, antibody to Gal4-AD from Clontech, antibodies to GFP, GAPDH, Alexa 555-conjugated Tf, Alexa 555-conjugated WGA, streptavidin-horseradish peroxidase (HRP) and Alexa 488-, 555- and 647-conjugated secondary antibodies from Life Technologies, pLKO-derived plasmids with shRNA sequence (shLuc, shAP2M1: TRCN0000060242, shAP3D1: TRCN0000065096) from Sigma Aldrich, Yeast reagents: yeast extract-peptone-dextrose from Sigma Aldrich, all the other powder media and amino acids mix from MP Biomedicals

Generation of yeast two-hybrid constructs, yeast two-hybrid assay and preparation of yeast lysates

All the Gal4bd (DNA-binding domain of Gal4) fusion constructs were synthesized by ligating annealed synthetic oligonucleotides (fusion proteins corresponding to the sequences of the various targeting signal peptides are listed in Table S1) into the *Eco*RI and *Bam*HI sites of pLex10. Constructs in pGad-derived vectors (pACT2 or pGAD-S2X) having the Gal4ad (activating domain of Gal4) fused to μ1-, μ2-, μ3-, μ4- or α-adaptin were kindly provided by J. Bonifacino (16,30,31).

The *Saccharomyces cerevisiae* L40 strain (MATa, his3-delta200 trp1-901 leu2-3, 112 ade2, lys2-801 am, LYS2::(lexAop)4-HIS3, URA3::(lexAop)8-lacZ GAL4) was maintained at 30°C and transformed by a rapid LiAc method (32). The 1.5 mL liquid yeast culture was grown overnight in YPD medium. After centrifugation of yeast culture, 100 μg of boiled salmon sperm carrier DNA with a pair of pGAD-based and pLex-based plasmids (1 μg of each, see above) were added to the yeast pellets that were further resuspended in a mix of 40% polyethylene glycol, 0.1 M LiAc and 10× Tris−ethylenediaminetetraacetic acid. Subsequently, dimethyl sulfoxide (DMSO) was added to a final concentration of 10% and yeasts were incubated for 30 min at room temperature with regular mixing. After a heat-shock (15 min at 42°C), transformants were plated onto Dropout Base (DOB) medium lacking tryptophan and leucine (DO-L-T) to select for colonies containing both plasmids and grown at 30°C. Three colonies for each combination of plasmids were picked and grown for 3–4 days on fresh DO-L-T, and were then replicated on the DO-L-T histidine limiting solid medium and on a solid DO-L-T medium with a circular Whatman filter for a β-galactosidase assay and analyzed after additional 3–4 days of growth. Whatman filters with yeast transformants were frozen in liquid nitrogen and incubated in 3 mL of Z buffer

(60 mM Na$_2$HPO$_4$·7H$_2$O, 40 mM, NaH$_2$PO$_4$·H$_2$O, 10 mM KCl and 1 mM MgSO4·7H$_2$O) with 1.2 mg of X-Gal and 0.6 % of β-mercaptoethanol at 30°C overnight.

The yeast total cell lysates were prepared according to the post-alkaline extraction protocol (33). Four milliliters of DOB media lacking trypto-phan was inoculated with yeast colonies transformed (as described above) with pGAD-derived constructs. After overnight incubation at 30°C with shaking, about 2.5 OD$_{600}$ of yeast cells were spun down for 5 min at 2790 g. The yeast pellets were resuspended in 100 µL of distilled water and incu-bated with 0.1 M NaOH for 5 min at room temperature. After 3 min cen-trifugation at 2790 g, the pellet was resuspended in 50 µL of 2× Laemmli sample buffer, heated 3 min at 95°C, centrifuged 3 min at 2790 g and 20 µL was resolved by SDS–PAGE on 4–20 % gradient gel (Biorad) and ana-lyzed by immunoblotting with anti-Gal4-AD antibody.

Cell lines and cell culture

HeLa cells (ATCC) were grown in DMEM supplemented with 10% fetal calf serum, 100 units/mL penicillin, 0.1 mg/mL streptomycin and 2 mM L-glutamine. *HeLa* cells transduced with lentiviral vectors compris-ing short hairpin RNA to luciferase, µ2 and δ subunits of APs were main-tained in DMEM supplemented as described above and with 1 µg/mL of puromycin.

To generate the stable shAP-2, shAP-3 and shLuc *HeLa* cell line lentiviruses were produced in HEK293T cells by co-transfecting pLKO-Puro-derived constructs comprising shRNAs (Table S2) together with pMDL, pREV and pVSVG helper vectors as described (34). *HeLa* cells were transduced by lentiviral particles containing shRNA at a multiplicity of infection of 3.5 in the presence of 8 µg/mL of polybrene.

Generation of EGFP fusion constructs and transfection of *HeLa* cells

The constructs for the expression of the GFP-tagged WT cystinosin and its mutant forms (ΔYFPQA-EGFP and ΔGYDQL-EGFP) have been previously described (4). The full-length cDNA encoding the WT human CD63 was kindly provided by Michael J. Caplan (25) and subsequently subcloned into the EGFP-C3 vector (Clontech). The WT CD63 was then modified to replace the last 10 amino acids of CD63 with the tail of cystinosin. The CD63-cystinosin chimera (EGFP-CD63-Cter) was gen-erated using a 5′ primer complementary to the N-terminal sequence of human CD63 (5′-CCGCTCGAG ATGGCGGTGGAAGGAGG-3′) and a 3′ primer containing the C-terminal sequence of cystinosin (tail with the lysosomal sorting signal, RKRPGYDQLN) linked to 9 bp of CD63 (5′-CG GGATCCCGCTAGTTCAGCTGGTCATACCCCGGTCTCTTTCTCAC GAGGCAGCAGG-3′). The product was subsequently subcloned into the *Xho*I and *Bam*HI sites of the EGFP C3 plasmid.

For IF analysis and cell surface biotinylation, WT or shRNA-transduced *HeLa* cells were plated in six-well tissue culture dishes at 650 000 cells/dish with (for IF) or without (for cell surface biotinylation) glass coverslips. The day after, at 90% confluency, 2 µg of plasmid DNA was transfected with 6 µL of Lipofectamine 2000 reagent (Invitrogen) according to the

manufacturer's protocol in antibiotic-free medium. The medium was changed 5 h after transfection. Cells were used 20 h after transfection for analysis.

For TIRFM, shRNA-transduced *HeLa* cells were plated in the eight-well chamber prepared with sticky-Slide 8-well Ibidi system (Biovalley) with 65 000 cells/dish. The following day at 90% confluency, 0.2 µg of plas-mid DNA was transfected with 0.6 µL of Lipofectamine 2000 reagent as described above. Cells were used 20 h after transfection for analysis.

Quantification of cell surface levels of CD63, Lamp-1 and TfR by flow cytometry

For surface staining, 500 000 shRNA-transduced *HeLa* cells were har-vested, washed in ice-cold PBS and then labeled for 1 h at 4°C with the indicated primary antibody (1:100 anti-CD63 and 1:100 anti-Lamp-1 and 1:20 anti-TfR) with ice-cold PBS-1% BSA. After three washes in ice-cold PBS, cells were incubated for 1 h at 4°C with the secondary antibody (1:200) in ice-cold PBS-1% BSA. Cells were washed three times and resus-pended in ice-cold PBS-1% BSA to immediately perform flow cytometry on a three-color FACScalibur flow cytometer with the CELLQUEST software (BD Biosciences). Dead cells and debris were excluded by gating on for-ward/side light scatter, and 10 000 events, corresponding to cells positive for GFP, were analyzed per sample. The average expression level of pro-teins was determined by calculating the geomean fluorescence intensity. The cell surface levels of proteins in shAP-2 and shAP-3 cells were normal-ized to those in shLuc cells. Each bar represents the mean ± SEM from five experiments.

Tf uptake assay

Uptake of Tf-A555 (12 µg/mL) was followed in shRNA-transduced *HeLa* cells. A total of 80 000 cells were plated on glass coverslips and grown overnight in complete medium (10% FBS). The following day cells were washed in PBS, starved in DMEM-supplemented 100 units/mL penicillin, 0.1 mg/mL streptomycin and 2 mM L-glutamine and 0.5% BSA for 30 min at 37°C and then for 10 min at 4°C to block endocytosis. Uptake experi-ments were initiated by incubating the cells for 40 min at 4°C with fluo-rescent labeled Tf diluted in starvation medium. Cells were then washed three times with ice-cold PBS (to remove unbound ligands), incubated for 0, 5 or 10 min at 37°C in starvation medium. The cells were then rinsed once with PBS^{++}, fixed for 15 min with 4% paraformaldehyde in PBS at room temperature, rinsed twice with PBS^{++} and quenched for 10 min with 50 mM NH$_4$Cl in PBS^{++}. Glass coverslips were mounted on microscope slides using FLUOPREP (bioMatérieux®sa) and imaged on a LEICA SP8 laser scanning microscope system (Leica).

Cell surface biotinylation, immunoprecipitation and western blot

HeLa shLuc, shAP-2 or shAP-3 cells transiently expressing cystinosin-EGFP or its mutants (see above) were rinsed twice with ice-cold PBS^{++} (with 0.49 mM MgCl$_2$ and 0.9 mM CaCl$_2$) prior to cell surface biotinylation. All steps, unless stated otherwise, were performed

on ice and in the dark with shaking. Sulfo-NHS-LC-Biotin (Thermo Scientific) was resuspended in DMSO at 200 mg/mL and stocked up to 1 month in aliquots at −20°C. The cells were incubated with 50 μg/mL biotin in PBS^{++} for 30 min, rinsed twice with ice-cold PBS^{++}, quenched for 15 min with 50 mM NH_4Cl in PBS^{++}, rinsed twice with ice-cold PBS^{++} and incubated for 10 min with ice-cold lysis buffer [50 mM Tris, 150 mM NaCl, 1% Triton-X-100 and one tablet of Complete Protease Cocktail (Roche) per 50 mL]. Lysates were cleared by 10 min centrifugation at $1000 \times g$ at 4°C. The immunoprecipitations were performed using μMACS GFP Microbeads Isolation Kit (Miltenyi Biotec). Briefly, 25 μL of anti-GFP MicroBeads were incubated with 500 μL of lysate for 1 h at 4°C and then applied onto the μMACS separation columns. The protein isolation was further performed according to the manufacturer's recommendations. Fifty microliters of final eluates with precipitated proteins were divided into two, resolved by SDS–PAGE on 8% gel and analyzed by immunoblotting with streptavidin-HRP to detect the biotinylated fraction of precipitated proteins and anti-GFP antibody used for normalization. Levels of biotinylated fusion proteins were then determined by quantification of streptavidin:GFP ratio obtained from analyses of western blot signals for immunoprecipitated proteins from biotinylated samples. Statistical analysis using a Mann–Whitney test was performed with PRISM Version 5 (GraphPad software). The threshold for statistical significance was set to $p < 0.05$. Each bar represents the mean ± SEM from at least three experiments.

Immunofluorescence

HeLa cells were plated on glass coverslips in six-well tissue culture dishes at 400 000 or 600 000 cells/dish and transfected the following day. Twenty hours after transfection, the cells were rinsed once with PBS^{++}, fixed for 15 min with 4% paraformaldehyde in PBS at room temperature, rinsed twice with PBS^{++} and quenched for 10 min with 50 mM NH_4Cl in PBS^{++}. After rinsing twice with PBS^{++}, the slides were incubated with primary antibody in PBS^{++} containing 0.075% saponin, 0.1% BSA and 5% normal donkey or goat serum (depending on secondary antibody used) 1 h at room temperature or overnight at 4°C, rinsed three times with PBS^{++}, incubated with secondary antibodies produced in donkey or goat (diluted 1:200 in PBS^{++} with 0.075% saponin, 0.1% BSA and 5% normal donkey or goat serum) for 1 h at room temperature and washed three times with PBS^{++} Glass coverslips were mounted on microscope slides using FLU-OPREP (bioMatérieux®sa) and imaged on a LEICA SP8 laser scanning microscope system (Leica).

Colocalization analysis

Confocal optical slices were captured using a 63× oil objective lens (Leica Microsystems), an optical slice thickness of 800 nm, a Z-step size of 400 nm and X-Y pixel size of 71 nm (Leica SP5 confocal microscope). The *trans*-Golgi region and early endosomal compartment were defined by delimiting TGN46- or EEA1-labeled area, respectively, using the IMAGEJ 1.47 software. The Golgi or early endosomal accumulation of cystinosin-EGFP or EGFP-CD63-Cter was measured as a percentage of the TGN46- or EEA1-labeled area which colocalized with GFP fusion proteins. Statistical analysis using a Mann–Whitney test was performed with

PRISM Version 5 (GraphPad software). The threshold for statistical significance was set to $p < 0.05$. Each bar represents an average of at least 20 cells.

Total internal reflection fluorescence assay

TIRFM assay was performed on *HeLa* shLuc and *HeLa* shAP-3 cells transfected with pDs-Red-Monomer-F (Clontech) together with cystinosin- or CD63-derived EGFP fusion proteins. The expression of farnesylated monomeric red fluorescent protein that remains bound to the PM was used as a general marker of the PM during image acquisition. Cells were placed within a temperature-controlled enclosure for live-cell imaging set at 37°C with 5% of CO_2. Fluorescence data were acquired with the Nikon Eclipse Ti-E TIRF imaging system (Nikon). The epifluorescent system enabled to select cells on the basis of their EGFP fluorescence. These cells were further processed in the TIRF system. First, the PM was delimited on the basis of the DsRed fluorescence and finally the EGFP TIRF image was acquired and used for the analysis. Images were recorded with the Nikon Ropper scientific QuanTEM 512 SC camera (Nikon) and analyzed with the NIS-ELEMENTS AR software (Version 3.1). Image sets were processed with the IMAGEJ Version 1.47 software. Mean corrected total cell surface fluorescence (mean CTCF) was calculated using this formula (35):

$$\text{Mean CTCF} = \text{CTCF/area of selected cell}$$

$$\text{CTCF} = \text{Integrated density} - (\text{area of selected cell} \\ \times \text{mean fluorescence of background readings}).$$

Statistical analysis using a Mann–Whitney test was performed with PRISM Version 5 (GraphPad software). The threshold for statistical significance was set to $p < 0.05$. Each bar represents the mean ± SEM for at least 10 cells.

Acknowledgments

GA#201590) and the 'Agence Nationale de la Recherche' (ANR) (Investments for the Future program - ANR-10-IAHU-01).

Supporting Information

Additional Supporting Information may be found in the online version of this article:

Figure S1. Analysis of growth of yeast colonies on histidine restricted medium. Yeast cells were co-transformed with bait constructs (Gal4bd fusion) containing triple repeats of the tyrosine-based motif of Lamp-1 (AGYQTI), CD63 (SGYEVM), cystinosin (PGYDQL, PGYDQLN) or its mutated form (PGADQLN) together with empty prey constructs (Gal4ad).Selection in the absence of histidine alone was not sufficient to eliminate growth of the yeasts transformed with the ((SGYEVM)x3), ((PGYDQL)x3) and ((PGYDQLN)x3) constructs. Growth of these transformants was blocked by addition of 3-AT (2.5 mM), a competitive inhibitor of histidine biosynthesis.

Figure S2. Cystinosin localizes to the late endosomal-lysosomal compartment in *HeLa* cells. *HeLa* cells were transfected with cystinosin-EGFP and co-labeled with anti-Lamp-1 or anti-CD63 antibodies (confocal microscopy; scale bars = 10 μm). The percentage of colocalization between cystinosin-EGFP and Lamp-1 or CD63 was analyzed with the IMAGEJ 1.47 software.

Figure S3. AP-2 and AP-3 depletion in *HeLa* cells. A and B) The expression of δ, γ, μ2 and α subunits of AP complexes in *HeLa* cells transduced with lentiviral particles containing shAP-2 (μ2), shAP-3 (δ) or shLuciferase (shLuc) was analyzed by WB (A) and IF (B) (scale bars = 10 μm). We obtained ~75% depletion of both δ and μ2 subunits (A). Lack of IF staining for the α subunit indicates that the remaining subunits of the AP-2 complex are not stable after μ2 depletion. C and D) Effects of AP-2 and AP-3 depletion on cell surface levels of CD63, Lamp-1 and TfR. C) The cell surface levels of CD63, Lamp-1 and TfR in shAP-2 and shAP-3 cells analyzed by flow cytometry were normalized to those of shLuc cells ($n = 5$); fluorescence-activated cell sorter (FACS) profiles of the cell surface expression of CD63, Lamp-1 and TfR in *HeLa* shLuc (blue), shAP-2 (green) and shAP-3 (red) cells from one representative experiment are shown. D) Analysis of uptake of Alexa555-conjugated Tf in shLuc, shAP-2 and shAP-3 cells. Cells were incubated at 4°C with Alexa555-conjugated Tf, washed and then shifted at 37°C for the indicated period before fixation and analyzed by confocal microscopy. After 5 or 10 min, Tf was internalized in control and AP-3-depleted cells, whereas it remained at the cell surface in shAP-2 cells (scale bars = 10 μm).

Figure S4. Image acquisition by TIRFM. *HeLa* shLuc cells were co-transfected with farnesylated monomeric DsRed (DsRed-Monomer-F) and cystinosin-EGFP encoding plasmids and live cells were directly analyzed by TIRFM and epifluorescence under the same microscope (Nikon). DsRed was used as a control for cell surface staining and expression of cystinosin was verified by epifluorescence (scale bars = 10 μm).

Table S1. List of fusion proteins used for the yeast two-hybrid assay

Table S2. Sequences of shRNAs used in the study

Table S3. List of EGFP fusion proteins used for the transfection

References

1. Jezegou A, Llinares E, Anne C, Kieffer-Jaquinod S, O'Regan S, Aupetit J, Chabli A, Sagne C, Debacker C, Chadefaux-Vekemans B, Journet A, Andre B, Gasnier B. Heptahelical protein PQLC2 is a lysosomal cationic amino acid exporter underlying the action of cysteamine in cystinosis therapy. Proc Natl Acad Sci U S A 2012;109:E3434–E3443.
2. Town M, Jean G, Cherqui S, Attard M, Forestier L, Whitmore SA, Callen DF, Gribouval O, Broyer M, Bates GP, van't Hoff W, Antignac C. A novel gene encoding an integral membrane protein is mutated in nephropathic cystinosis. Nat Genet 1998;18:319–324.
3. Gahl WA, Thoene JG, Schneider JA. Cystinosis. N Engl J Med 2002;347:111–121.
4. Cherqui S, Kalatzis V, Trugnan G, Antignac C. The targeting of cystinosin to the lysosomal membrane requires a tyrosine-based signal and a novel sorting motif. J Biol Chem 2001;276:13314–13321.
5. Schroder B, Wrocklage C, Pan C, Jager R, Kosters B, Schafer H, Elsasser HP, Mann M, Hasilik A. Integral and associated lysosomal membrane proteins. Traffic 2007;8:1676–1686.
6. Schroder BA, Wrocklage C, Hasilik A, Saftig P. The proteome of lysosomes. Proteomics 2010;10:4053–4076.
7. Bonifacino JS, Traub LM. Signals for sorting of transmembrane proteins to endosomes and lysosomes. Annu Rev Biochem 2003;72:395–447.
8. Kyttala A, Ihrke G, Vesa J, Schell MJ, Luzio JP. Two motifs target Batten disease protein CLN3 to lysosomes in transfected nonneuronal and neuronal cells. Mol Biol Cell 2004;15:1313–1323.
9. Hirst J, Irving C, Borner GH. Adaptor protein complexes AP-4 and AP-5: new players in endosomal trafficking and progressive spastic paraplegia. Traffic 2013;14:153–164.
10. Hirst J, Barlow LD, Francisco GC, Sahlender DA, Seaman MN, Dacks JB, Robinson MS. The fifth adaptor protein complex. PLoS Biol 2011;9:e1001170.
11. Ihrke G, Kyttala A, Russell MR, Rous BA, Luzio JP. Differential use of two AP-3-mediated pathways by lysosomal membrane proteins. Traffic 2004;5:946–962.
12. Rous BA, Reaves BJ, Ihrke G, Briggs JA, Gray SR, Stephens DJ, Banting G, Luzio JP. Role of adaptor complex AP-3 in targeting wild-type and mutated CD63 to lysosomes. Mol Biol Cell 2002;13:1071–1082.
13. Robinson MS. Adaptable adaptors for coated vesicles. Trends Cell Biol 2004;14:167–174.
14. Stephens DJ, Banting G. Specificity of interaction between adaptor-complex medium chains and the tyrosine-based sorting motifs of TGN38 and lgp120. Biochem J 1998;335:567–572.
15. Sekiguchi T, Hirose E, Nakashima N, Ii M, Nishimoto T. Novel G proteins, Rag C and Rag D, interact with GTP-binding proteins, Rag A and Rag B. J Biol Chem 2001;276:7246–7257.
16. Ohno H, Fournier MC, Poy G, Bonifacino JS. Structural determinants of interaction of tyrosine-based sorting signals with the adaptor medium chains. J Biol Chem 1996;271:29009–29015.
17. Bonifacino JS, Dell'Angelica EC. Molecular bases for the recognition of tyrosine-based sorting signals. J Cell Biol 1999;145:923–926.

18. Janvier K, Bonifacino JS. Role of the endocytic machinery in the sorting of lysosome-associated membrane proteins. Mol Biol Cell 2005;16:4231–4242.

19. Berger AC, Salazar G, Styers ML, Newell-Litwa KA, Werner E, Maue RA, Corbett AH, Faundez V. The subcellular localization of the Niemann-Pick Type C proteins depends on the adaptor complex AP-3. J Cell Sci 2007;120:3640–3652.

20. Lefrancois S, Janvier K, Boehm M, Ooi CE, Bonifacino JS. An ear-core interaction regulates the recruitment of the AP-3 complex to membranes. Dev Cell 2004;7:619–625.

21. Salazar G, Craige B, Styers ML, Newell-Litwa KA, Doucette MM, Wainer BH, Falcon-Perez JM, Dell'Angelica EC, Peden AA, Werner E, Faundez V. BLOC-1 complex deficiency alters the targeting of adaptor protein complex-3 cargoes. Mol Biol Cell 2006;17:4014–4026.

22. Rappoport JZ, Simon SM. Real-time analysis of clathrin-mediated endocytosis during cell migration. J Cell Sci 2003;116:847–855.

23. Dugast M, Toussaint H, Dousset C, Benaroch P. AP2 clathrin adaptor complex, but not AP1, controls the access of the major histocompatibility complex (MHC) class II to endosomes. J Biol Chem 2005;280:19656–19664.

24. Chen J, Wang J, Meyers KR, Enns CA. Transferrin-directed internalization and cycling of transferrin receptor 2. Traffic 2009;10:1488–1501.

25. Duffield A, Kamsteeg EJ, Brown AN, Pagel P, Caplan MJ. The tetraspanin CD63 enhances the internalization of the H,K-ATPase beta-subunit. Proc Natl Acad Sci U S A 2003;100:15560–15565.

26. Ohno H, Aguilar RC, Yeh D, Taura D, Saito T, Bonifacino JS. The medium subunits of adaptor complexes recognize distinct but overlapping sets of tyrosine-based sorting signals. J Biol Chem 1998;273:25915–25921.

27. Taranta A, Petrini S, Palma A, Mannucci L, Wilmer MJ, De Luca V, Diomedi-Camassei F, Corallini S, Bellomo F, van den Heuvel LP, Levtchenko EN, Emma F. Identification and subcellular localization of a new cystinosin isoform. Am J Physiol Renal Physiol 2008;294:F1101–F1108.

28. Peden AA, Oorschot V, Hesser BA, Austin CD, Scheller RH, Klumperman J. Localization of the AP-3 adaptor complex defines a novel endosomal exit site for lysosomal membrane proteins. J Cell Biol 2004;164:1065–1076.

29. Liu B, Du H, Rutkowski R, Gartner A, Wang X. LAAT-1 is the lysosomal lysine/arginine transporter that maintains amino acid homeostasis. Science 2012;337:351–354.

30. Ohno H, Stewart J, Fournier MC, Bosshart H, Rhee I, Miyatake S, Saito T, Gallusser A, Kirchhausen T, Bonifacino JS. Interaction of tyrosine-based sorting signals with clathrin-associated proteins. Science 1995;269:1872–1875.

31. Aguilar RC, Boehm M, Gorshkova I, Crouch RJ, Tomita K, Saito T, Ohno H, Bonifacino JS. Signal-binding specificity of the mu4 subunit of the adaptor protein complex AP-4. J Biol Chem 2001;276:13145–13152.

32. Gietz RD, Schiestl RH. Quick and easy yeast transformation using the LiAc/SS carrier DNA/PEG method. Nat Protoc 2007;2:35–37.

33. Kushnirov VV. Rapid and reliable protein extraction from yeast. Yeast 2000;16:857–860.

34. Dull T, Zufferey R, Kelly M, Mandel RJ, Nguyen M, Trono D, Naldini L. A third-generation lentivirus vector with a conditional packaging system. J Virol 1998;72:8463–8471.

35. Gavet O, Pines J. Progressive activation of CyclinB1-Cdk1 coordinates entry to mitosis. Dev Cell 2010;18:533–543.